

# A Monte Carlo Generator for Full Simulation of $e^+e^- \rightarrow \text{hadrons}$ Cross Section Scan Experiment

D. Zhang, G. Rong, J.C. Chen

*Institute of High Energy Physics, Beijing 100049, China*

## Abstract

A generator with  $\alpha^2$  order radiative correction effects, including both the initial state radiative corrections and the photon vacuum polarization corrections, is built for the full simulation of  $e^+e^- \rightarrow \text{hadrons}$  in cross section scan experiment in the quarkonium energy region. The contributions from the hadron production structures including the resonances of  $1^{--}$  quarkonium families and the light hadrons spectrum below 2 GeV as well as the QED continuum hadron spectrum are all taken into account in the event generation. It was employed successfully to determine the detection efficiency for selection of the events of  $e^+e^- \rightarrow \text{hadrons}$  from the data taken in the energy region from 3.650 GeV to 3.872 GeV covering both the  $\psi(3686)$  and  $\psi(3770)$  resonances in BES experiment. The generator reproduces the properties of hadronic event production and inclusive decays well.

## 1 Introduction

$\psi(3770)$  is the charmonium resonance with the lowest mass above open charm-pair threshold. It is thought to decay almost entirely to  $D\bar{D}$  [1]. However, it has been a puzzle for a long time that some measured values of  $D\bar{D}$  production cross section  $\sigma_{D\bar{D}}$  at the peak of  $\psi(3770)$  resonance fail to fit in the measured values of the cross section  $\sigma_{\psi(3770)}$  for  $\psi(3770)$  production at the peak. The discrepancy between the  $\sigma_{\psi(3770)}$  and  $\sigma_{D\bar{D}}$  was historically found to be more than 30% [2] [3]. To understand this long-standing puzzle, it is crucial to measure the  $\psi(3770)$  resonance parameters and the  $D\bar{D}$  cross section at the resonance peak precisely in the same experiment. Experimentally,  $\psi(3770)$  resonance parameters are extracted from fitting the observed hadronic cross sections in the energy range which covers the  $\psi(3770)$  resonance in cross section scan experiment. However, since the  $\psi(3686)$  resonance is closed to the  $\psi(3770)$ , and the cross section of continuum QED production exceeds the contribution of  $\psi(3770)$  resonance the heavy overlaps between them would affect the cross section configuration in this energy region. In order to accurately measure the parameters of the resonances one had better simultaneously to deal with both the resonances and the contribution of continuum production based on the same data set. So, the determinations of the efficiencies for detecting the inclusive hadronic events point by point is necessary in the energy region covering several production processes.

The determinations of efficiencies for detecting the  $e^+e^- \rightarrow \text{hadrons}$  events in such energy region would be more complicate than that in the case for which only single narrow resonance has been concerned in the data taking, in which the initial state radiation (ISR) effect and the continuum contribution are negligible small, or in the case of the simple R value measurement in the  $e^+e^-$  annihilation in the energy region far away from any resonances. Due to the ISR effects, the actual energy to produce final products would drop to rather wide region below the collision energy by photon emissions from the beam particles. The detector response, the composition of the different physical processes in the whole region and even the event selection criteria all vary with the energies and finally affect the detection efficiency at the collision energy points. To obtain the efficiencies at each of the different energy points reliably, a generator to produce the full processes of  $e^+e^- \rightarrow \text{hadrons}$  is developed.

Sometimes for convenience the contribution from the vacuum polarization can be turned off in the event generation. The possible interferences between the continuum hadron production and the inclusive electro-magnetic (EM) decay mode of narrow resonances are considered in the generator and can be turned on/off too.

## 2 Method

### 2.1 Radiative correction in $e^+e^-$ annihilation

Due to ISR, the actual c.m. energy of the inclusive hadron system produced in the  $e^+e^-$  annihilation is  $\sqrt{s'} = \sqrt{s(1-x)}$ , where  $\sqrt{s}$  is the collision center-of-mass energy, and  $x(1 > x \geq 0)$  is a parameter relating to the total energy of the emitted photons [5].

Fig. 1 shows the differential cross section of the hadron production with respect to  $\sqrt{s'} = \sqrt{s(1-x)}$  for the case of that the nominal center-of-mass energy is set to 3.80 GeV. To  $\alpha^2$  order radiative correction in  $e^+e^-$  annihilation, the differential cross section of hadron production with respect to the hard photon energy parameter  $x$ , instead of  $\sqrt{s'}$  can be written as

$$\frac{d\sigma^{exp}(s)}{dx} = \frac{\sigma^0[s(1-x)]}{|1 - \Pi[s(1-x)]|^2} F(x, s), \quad (1)$$

where  $F(x, s)$  is a sampling function for the radiative photon energy fraction  $x$ . Neglecting the  $Z^0$  exchange contributions in the structure function approach introduced by Kuraev and Fadin [5], it can be written as

$$F(x, s) = \beta x^{\beta-1} \delta^{V+S} + \delta^H, \quad (2)$$

in which  $\beta$  is the electron equivalent radiator thickness,

$$\beta = \frac{2\alpha}{\pi}(L-1)$$

and

$$L = \ln \frac{s}{m_e^2}$$

where  $m_e$  is the mass of electron,  $\alpha$  is the fine structure constant, and

$$\delta^{V+S} = 1 + \frac{3}{4}\beta + \frac{\alpha}{\pi}\left(\frac{\pi^2}{3} - \frac{1}{2}\right) + \frac{\beta^2}{24}\left(\frac{37}{4} - \frac{L}{3} - 2\pi^2\right), \quad (3)$$

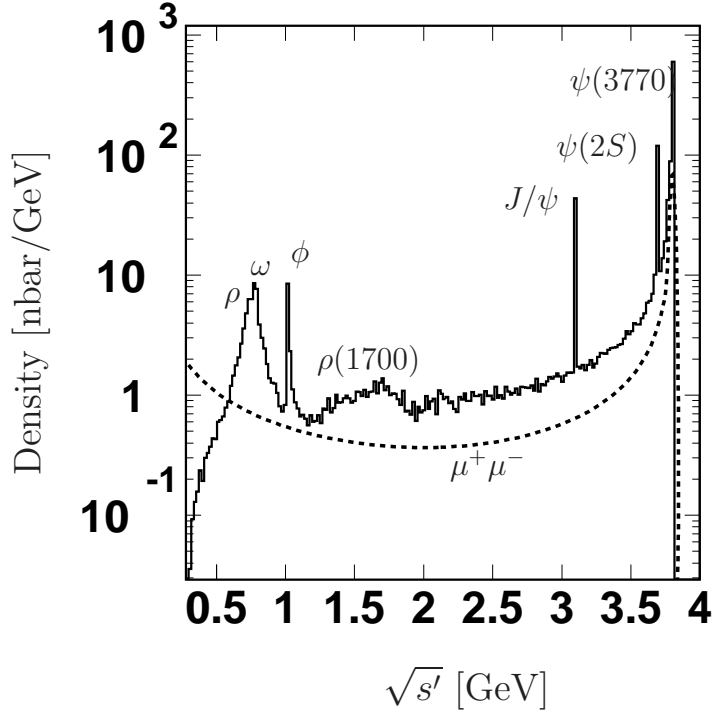


Figure 1: The differential hadron production cross section due to ISR return with respect to the actual c.m. energy  $\sqrt{s'}$ ,  $d\sigma^{exp}(s)/d\sqrt{s'}$  in the case that the nominal collision center-of-mass energy is set to  $\sqrt{s} = 3.80$  GeV. The dashed line shows the differential cross section for  $\mu^+\mu^-$  production.

$$\delta^H = \delta_1^H + \delta_2^H, \quad (4)$$

in which

$$\delta_1^H = -\beta(1 - \frac{x}{2})$$

and

$$\delta_2^H = \frac{1}{8}\beta^2[4(2-x)\ln\frac{1}{x} - \frac{1+3(1-x)^2}{x}\ln(1-x) - 6+x].$$

In Eq. (1),  $1/|1 - \Pi[s(1-x)]|^2$  is the vacuum polarization correction factor including both the leptonic and the hadronic terms i.e.

$$\Pi(s) = \Pi_h(s) + \Pi_l(s) \quad (5)$$

in which

$$\Pi_h(s) = \frac{s}{4\pi^2\alpha}[PV \int \frac{\sigma^0(s')}{s-s'}ds' - i\pi\sigma^0(s)]$$

and

$$\Pi_l(s) = \frac{\alpha}{\pi}f(\xi),$$

where

$$f(\xi) = -\frac{5}{9} - \frac{\xi}{3} + \frac{\sqrt{1-\xi}(2+\xi)}{6} \ln\left[\frac{1+\sqrt{1-\xi}}{1-\sqrt{1-\xi}}\right] \quad (\xi \leq 1)$$

and

$$f(\xi) = -\frac{5}{9} - \frac{\xi}{3} + \frac{\sqrt{1-\xi}(2+\xi)}{3} \tan^{-1} \frac{1}{\sqrt{\xi-1}} \quad (\xi > 1),$$

in which  $\xi = \frac{4m_l^2}{s}$  where  $m_l$  is the mass of lepton  $l$  ( $l = e, \mu, \tau$ ). In Eq. (1),

$$\sigma^0[s(1-x)] = \frac{4\pi\alpha^2}{3s(1-x)} R + \sum_i \sigma_{res,i}^0[s(1-x)] \quad (6)$$

is the total lowest order cross-section at  $\sqrt{s'} = \sqrt{s(1-x)}$  in which  $R$  is the ratio of continuum hadron cross section to the cross section of  $e^+e^- \rightarrow \mu^+\mu^-$ , and

$$\sigma_{res,i}^0[s(1-x)] = \frac{12\pi\Gamma_{h,i}\Gamma_{ee,i}^0}{[s(1-x) - (M_i^0)^2]^2 + (M_i^0)^2\Gamma_i^2} \quad (7)$$

is the lowest order cross section of the  $i$ th resonance, where  $\Gamma_{ee,i}^0$ ,  $M_i^0$ ,  $\Gamma_{h,i}$  and  $\Gamma_i$  are the lowest order leptonic width, the lowest order mass, the hadronic width and the total width of the  $i$ th resonance, and ' $i$ ' denote the  $i$ th. resonance of the  $1^{--}$  quarkonium states and the states with mass below 2 GeV/ $c^2$ . For wide resonances the widths  $\Gamma_i$ 's and  $\Gamma_{h,i}$  vary with energy depending on their decay products.

In Fig. 2 a), the solid line shows the total lowest order cross section for inclusive hadronic event production in the region from 3.65 GeV to 4.0 GeV including the five processes:  $e^+e^- \rightarrow J/\psi$ ,  $e^+e^- \rightarrow \psi(3686)$ ,  $e^+e^- \rightarrow \psi(3770)$ ,  $e^+e^- \rightarrow \psi(4040)$  and  $e^+e^- \rightarrow \gamma^* \rightarrow hadrons$ ; while the dashed line shows the expected total cross section with the radiative corrections for the inclusive hadron production. These cross sections are generated with the generator. In Fig. 2 b), the contributions of the radiatively corrected cross sections of the five processes are demonstrated, respectively. The energy spread for generating the events is set to be zero.

The ratio of the expected observation cross section to the lowest order cross section, see the two lines in Fig. 2 a) is the radiative correction factor for the inclusive  $e^+e^- \rightarrow hadrons$  process

$$1 + \delta = \frac{\sigma^{exp}(s)}{\sigma^0(s)}, \quad (8)$$

which is shown in Fig 2 c).

From Fig. 2 c) one can see that the radiative correction effects vary rather large around the resonance. Except for the ISR corrections, under the narrow resonance peak the large real and imaginary part of vacuum polarization correction would shift the lowest order resonance peak position  $M^0$  up by an amount of

$$\Delta M = \frac{\frac{3}{2\alpha}\Gamma_{ee}^0 + \frac{\alpha}{6}R\Gamma}{1 - Re\Pi'[(M^0)^2]}, \quad (9)$$

where  $R$  denotes the  $R$  value for the continuum hadron production and  $\Pi'[(M^0)^2]$  denotes the vacuum polarization function from all the contributions of leptons and hadrons except for the contribution from the resonance itself at the position  $s = (M^0)^2$ . And

$$M = M^0 + \Delta M \quad (10)$$

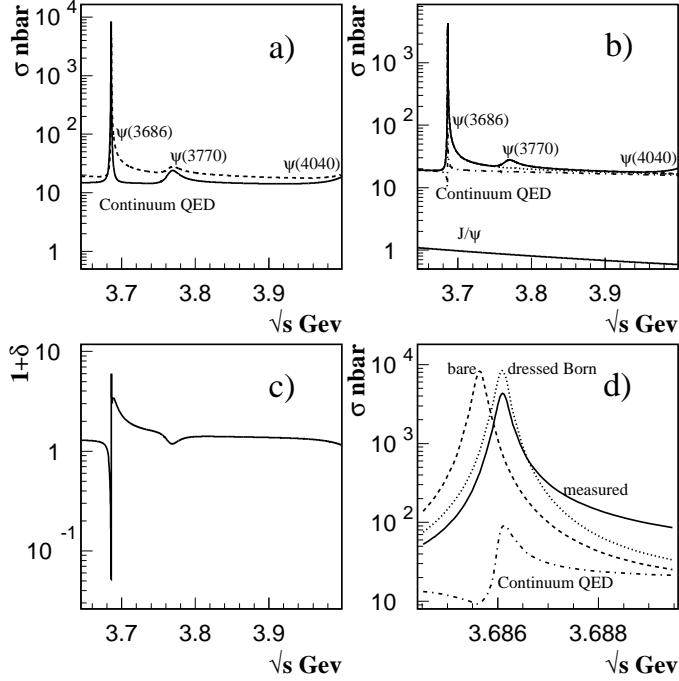


Figure 2: The cross sections of  $e^+e^-$  annihilation into inclusive hadron in the energy region from 3.65 GeV to 4.0 GeV. a) shows the total lowest order cross section (solid line) and the expected total cross section in the region, produced by the generator with null collision energy spread setting (dashed line); b) demonstrates the respective contributions of the expected cross sections of the five processes mentioned in the text; c) represents the radiative correction factor  $1 + \delta$ ; and d) gives some detail information about the radiative corrections at the position of the sharp resonance  $\psi(3686)$  in the tiny energy window from 3.6845 GeV to 3.6895 GeV. The EM interference effect between  $\psi(3686)$  and continuum QED is turned off in the event generation.

is the observable peak position of the resonance related to the single photon exchange processes. One can also dress the lowest order leptonic width  $\Gamma_{ee}^0$  to the physical one  $\Gamma_{ee}$  in the same way, by

$$\Gamma_{ee} = \frac{\Gamma_{ee}^0}{|1 - Re\Pi'[(M^0)^2]|^2}, \quad (11)$$

for calculation of  $d\sigma^{exp}(s)/dx$  given in Eq. (1). The change of the total width  $\Gamma$  due to the vacuum polarization is negligibly small. The dashed line and dotted line in Fig. 2 d) show the split of  $\psi(3686)$  peak due to the EM vacuum polarization given in Eq. (9). The label 'bare' in Fig. 2 d) indicate the lowest order peak position which can be seen in the processes in which there are no EM effects infected.

The vacuum polarization effects also cause the flat continuum QED contribution vibration under the sharp resonance, which is shown by dashed dotted line in Fig. 2 d) and also in Fig. 3 b) by the red line. The solid line in Fig. 2 d) represents the expected total cross section in the energy region.

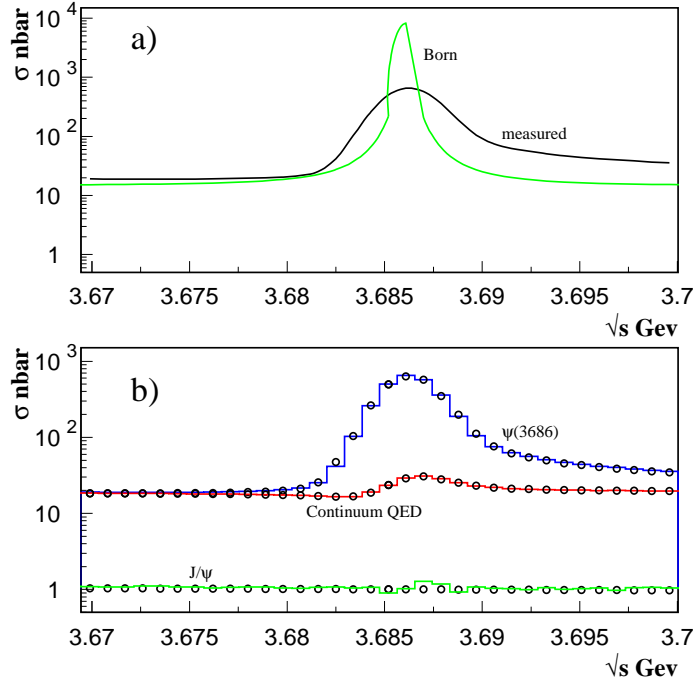


Figure 3: The simulation of a fine cross section scan in  $\psi(3686)$  resonance region where the energy spread is assumed to be 1.35 MeV. In a), the expected observation cross section is shown by the solid line, while the green line shows the lowest cross section; and in b) the contributions from the three observation cross sections, i.e. the  $J/\psi$  tail, the  $\psi(3686)$  and the continuum QED process, are demonstrated. The circle marks on the lines in b) represent the integrated results of Eq. (1) for the cross sections of the three processes.

Fig. 3 a) shows the different behavior of the lowest order cross section and the expected observable cross section due to radiative effects and with finite collision energy spread (1.35 MeV) generated with the generator in the  $\psi(3686)$  resonance region. While Fig. 3 b) shows the contributions of the observation cross sections of three relative processes in the energy region, the tail of  $J/\psi$ , the  $\psi(3686)$  resonance and the continuum QED, in which the vibration of the continuum QED line shape caused by the vacuum polarization corrections is still seen clearly in the finite energy spread case (the red line). The finite energy spread does drop the sharp resonance peak significantly but does not eliminate the vibration of continuum QED line shape as shown in the figure. If the data handling, the event selection, the determination of the detection efficiencies and the physical considerations of the hadron spectrum structure are all treated properly and correctly in the cross section scan experiments, one can expect that the vibration effects of continuum QED line shape due to vacuum polarization lying on the narrow resonance region would be observable.

The circle marks on the lines in Fig. 3 b) are the integrated numerical results of Eq. (1) for the corresponding cross sections. The accuracies of the simulated cross sections by the generator are quite good.

## 2.2 Sub-generators

From Fig. 1, one can see that the hadronic events not only be produced at the  $\sqrt{s}$ , but also produced in the full energy range from  $\sqrt{s}$  to 0.28 GeV, the two pion production threshold. To correctly simulate the full process produced in  $e^+e^-$  annihilation, the generator should be a mixture of sub-generators in which each single generator simulates a special processes and runs together with others, driving according to the ISR return energy spectrum weighted by the lowest order cross sections of the processes involved in the energy region. Up to the charmonium system energy region, these physics processes include one photon continuum hadron production,  $e^+e^- \rightarrow J/\psi, \psi(3686)$ , which decay to hadronic final states inclusively, the  $e^+e^- \rightarrow \psi(3770), \psi(4040)$  and  $\psi(4160)$  etc. which go to the hadron final states through the mediate charmed meson pairs inclusively. The production of  $1^{--}$  resonances at lower energy range are also included, such as the  $\rho(1700)$ ,  $\phi(1680)$ ,  $\omega(1650)$ ,  $\rho(1450)$ ,  $\omega(1420)$ ,  $\phi(1020)$ ,  $\omega(780)$  and  $\rho(770)$  etc.. Those states are arranged respectively to go to various final states such as  $\pi\pi, K\bar{K}, K\bar{K}\pi, 4\pi, 5\pi, 6\pi, \dots$  exclusively with their corresponding cross sections and branching fractions. The events of  $e^+e^- \rightarrow \gamma^* \rightarrow \text{hadrons}$  and the inclusive hadron decays of charmonium resonance  $\psi(3686)$  and  $J/\psi$  are generated by their respective inclusive LUND-type generators [6] [7]. While the events which decay from other resonances such as the  $\psi(3770)$ ,  $\phi(1680)$ ,  $\phi(1020)$ ,  $\rho(1700)$ ,  $\rho(1450)$ ,  $\rho(770)$  and  $\omega(782)$  etc. to all possible final states according to the known decay modes and branching fractions [4], can be generated by corresponding sub-generators conveniently. The Lorentz boost of the hadron system recoiling against the radiative photons are planted into the sub-generator's operation. A normal distribution random number generator has been employed to simulate the effects of energy spread at the collision energy  $\sqrt{s}$ .

### 2.3 Sampling Technique

From Eq. (7), Eq. (2) and Fig. 1 one can see that there are many sharp peaks, such as the  $J/\psi$ ,  $\psi(3686)$  peaks (see Fig. 1 and Fig. 2) and the sharp photon ISR spectrum at the singularity when  $x \rightarrow 0$  (equivalent to  $\sqrt{s'} \rightarrow 3.8$  GeV in Fig. 1), which enter into the probability distribution function given in Eq. (1). All of those sharp structures may slow greatly the Mont Carlo sampling procedure and affect the accuracy of the event generations, especially for the accuracies of the shapes of the sharp variation lines which are extremely important for the determination of the detection efficiencies. Sometimes people can eliminate the singularities by Monte Carlo inverse transformation techniques, but it is almost impossible to eliminate all those singularities simultaneously by an inverse transformation function. A special importance sampling method with multi-section scheme treatment has been developed in this work. One divides the whole of ISR return energy region into several sections to guarantee that for every section there is only one or less peak of the distribution function given by Eq. (1). Three kinds of sections are defined: 1) the resonance section in which there is only one sharp resonance like  $J/\psi$  or  $\psi(3686)$ ; 2) the slow varying sections in which there is no sharp resonance or any singularity; and 3) the section in which the ISR spectrum has the singularity i.e. the region which directly touches to the collision energy point  $x \rightarrow 0$ , ( $s' \rightarrow s$ ), for which the section range is variable and depending on the position of the nearest sharp resonance beneath the collision energy  $\sqrt{s}$ . When the collision energy with its energy spread range close to the narrow resonance or overlap each other, the width of the ISR singularity section  $x_0$  ( $x_0 \geq x \geq 0$ ) should ensure that both of the variation of the lowest order cross section in the singularity section region ( $x_0 \geq x \geq 0$ ) and the variation of the ISR spectrum in the touched sharp resonance section should be comparably moderate enough.

The sharp resonance peak in the resonance section can be eliminated easily by the inverse function transformation, defining the new variant  $\rho$  instead of  $x$ , in Eq. (1)

$$x = 1 - [M \cdot \Gamma \cdot \tan(\tan^{-1}(\frac{s(1 - x^{up}) - M^2}{M \cdot \Gamma}) - \Omega \cdot \rho) + M^2]/s, \quad (12)$$

in which

$$\Omega = \tan^{-1} \frac{s(1 - x^{up}) - M^2}{M \cdot \Gamma} - \tan^{-1} \frac{s(1 - x^{low}) - M^2}{M \cdot \Gamma}. \quad (13)$$

serves as the probability normalization constant in the transformation, and  $x_{up}$  and  $x_{low}$  are the up and low limits corresponding to the resonance section. The  $\rho$  is then the normalized random number taken uniformly from 0 to 1, which keeps the event production probability, i.e. the integrated area of Fig. 1 unchanged in the resonance section under the transformation. This transformation keeps the exact shape of the sharp resonance, but it blocks generating the initial state photons individually. It can just output the total energy and momentum of the emitted photons to serve for the Lorentz boost of the recoiling hadronic system. For the purpose of inclusive hadron measurement in  $e^+e^-$  collision experiment this simplification is feasible. The price paid here is worthy for the precise measurement of the narrow resonance parameters.

In this stage one can simply define the new normalized sampling random number  $\xi$  in (0,1) section instead of  $x$  to eliminate the singularity of the exponential ISR spectrum, the



leading logarithm term of Eq. (2) and keep the event production probability unchanged,

$$x = x_0 \xi^{1/\beta}, \quad (14)$$

where the  $\beta$  is as defined in Eq. (2), and the section width  $x_0$  here saves as the probability normalization constant in the transformation.

After performing the importance sampling procedure for the multi-section process according to the distribution of Eq. (1) and the normalized ratios of the lowest order cross sections of the processes involved to drive the corresponding sub-generators the Mont Carlo events will be then generated finally as mentioned in above section.

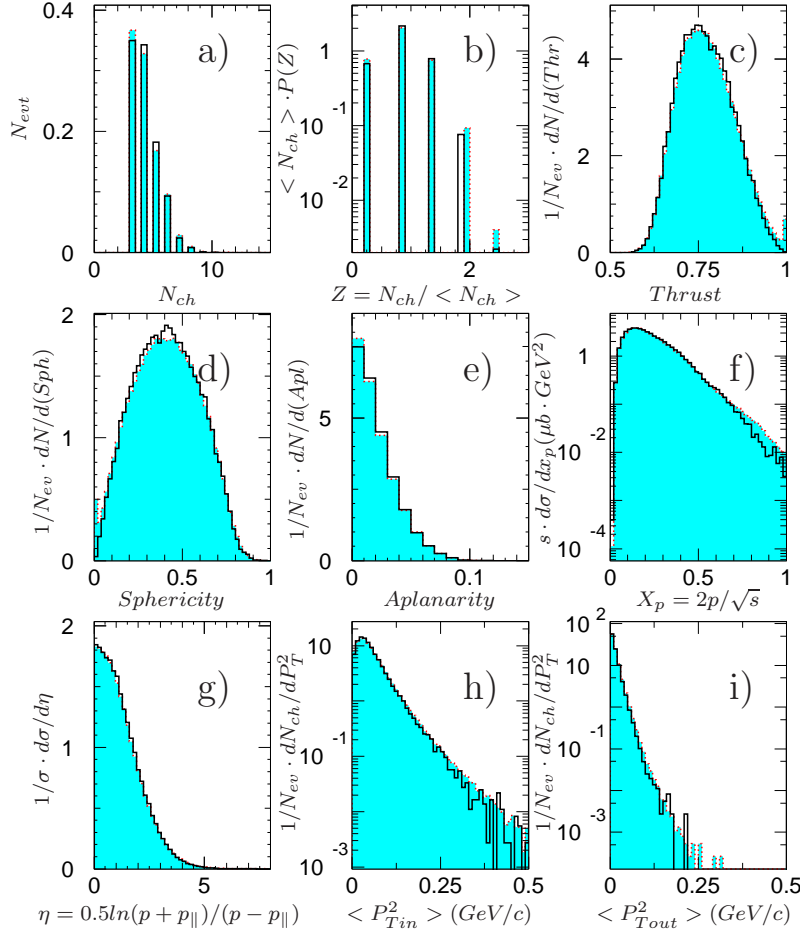


Figure 4: The properties of hadronic events produced at  $\sqrt{s} = 3.773$  GeV. Shadows are the distribution of experimental data [8], and lines are those generated with this generator; a) the charged multiplicity; b) the  $KNO$  scaling [10]; c) thrust [11], d) sphericity [12], e) aplanarity [12] f) Feynman scaling variable, g) pseudo-rapidity, h) and i) transverse momentum projection in and out the jet injection plane

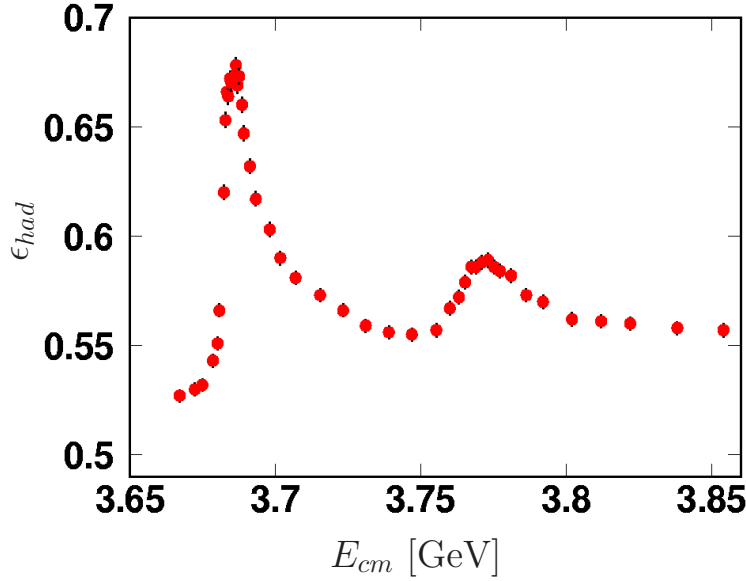


Figure 5: The efficiencies for detection of the inclusive hadronic events at each nominal center-of-mass energies.

### 3 Comparison with experiment data

Properties of hadronic events can be described by distributions of their kinematic variables. Fig. 4 show the distributions of kinematic variables of hadronic events produced at  $\sqrt{s} = 3.773$  GeV. In the figure, shadows show the distributions of the variables from data [8], and lines represent the distributions from Monte Carlo sample generated with this generator, in which the detector simulation is based on GEANT3 package [9]. In Fig. 4, a) is the charged multiplicity  $N_{ch}$  of events; b) is the  $KNO$  scaling distribution [10]; c), d) and e) are the thrust distribution [11], the sphericity distribution and aplanarity distribution of events [12], respectively; f) is the distribution of the Feynman scaling variable. Kinematic properties of hadronic events are described by g) pseudo-rapidity, and transverse momentum distributions h), n) and i). From Fig. 4 one can see that the qualities of the general simulation to the data are satisfied.

### 4 Application of the generator

Feeding the reconstructed Monte Carlo events for  $e^+e^- \rightarrow \text{hadrons}$  generated at each of the nominal center-of-mass energy points, at which the cross section scans were performed, into the analysis program to select the inclusive hadronic events one can determine the detection efficiencies  $\epsilon_{had}(s)$ . Fig. 5 shows the Monte Carlo efficiencies for detection of the hadronic events produced at the different nominal center-of-mass energies from 3.650 to 3.872 GeV. From the figure one can see that the efficiencies at the different energies with different physics processes involved are quite different. The efficiencies determined with the generator were used in the measurement of  $R$  values around 3.650 and at 3.773 GeV [13] which were used to extract the inclusive branching fractions of  $\psi(3770)$  decay to  $D\bar{D}$ , and in

the cross section scan experiment in the energy region covering both of  $\psi(3686)$  and  $\psi(3770)$  resonances performed with BES-II detector at the BEPC collider in Beijing [14]. For more precise measurements of the resonance parameters obtained by fitting the cross sections for inclusive hadron production in the energy range, where the complicate physical structure like the  $\psi(3686)$ ,  $\psi(3770)$  and  $\psi(4040)$  resonances involved, the correct determination of the detection efficiencies is crucial.

## 5 Conclusion

A new generator with  $\alpha^2$  order radiative correction for the full simulation of  $e^+e^- \rightarrow \text{hadron}$  process in the cross section scan experiment in the energy region covering multiple resonance structure is present. The complex resonances structure such as the  $\psi(3770)$ ,  $\psi(3686)$ ,  $J/\psi$ ,  $\psi(4040)$  and  $\psi(4160)$  as well as the continuum QED production and the resonances with masses below  $2 \text{ GeV}/c^2$ , are all included in the generator. The generator reproduces the properties of hadronic events very well and the detector efficiency can be determined conveniently for the hadronic cross section scan experiment.

## 6 Acknowledgment

This work is supported in part by the National Natural Science Foundation of China under contracts No. 10491304.

## References

- [1] W. Bacino *et al.*, (DELCO Collaboration), Phys. Rev. Lett. **40** 671 (1978).
- [2] G. Rong, (BES Collaboration), Presented at 39th Rencontres de Moriond on Electroweak Interactions and Unified Theories, La Thuile, Aosta Valley, Italy, 21-28 Mar. 2004, p401.
- [3] G. Rong, D. Zhang and J.C. Chen, arXiv:hep-ex/0506051.
- [4] S. Eidelman *et al.*, (Particle Data Group), Phys. Lett. **B592** 1 (2004).
- [5] E.A. Kuraev and V.S. Fadin, Yad Fiz, **41**, 377 (1985), [Sov. J. Nucl. Phys. **B41** 466 (1985)].
- [6] B. Andersson, G. Gustafson and T. Sjostrand, Z. Phys. **C6** 235 (1980); T. Sjostrand, Comput. Phys. Commun. **27** 243 (1982); **82** 74 (1994).
- [7] J.C. Chen *et al.*, Phys. Rev. **D 62** 034003 (2000).
- [8] J.C. Chen (BES Collaboration), Presented at International Conference on QCD and Hadronic Physics, Beijing, China, 16-20 June 2005.

- [9] CERN program library long writeup W5013, CERN, 1993; M. Ablikim et al, Nucl. Inst. and Meth. **A552** 344 2005.
- [10] Z. Koba, H.B. Nielsen and P. Olesen, Nucl. Phys. **B40** 317 (1972).
- [11] S. Brandt *et al.* Phys. Lett. **12** 57 (1964); E. Fahren, Phys. Rev. Lett. **39** 187 (1977).
- [12] J.D. Bjorken and S.J. Brodsky, Phys. Rev. **D1** 1416 (1970); R. Marshall, RAL-89-021 (1989).
- [13] G. Rong (BES Collaboration), Proceedings of the 11<sup>st</sup> International Conference on Hadron Spectroscopy, 2005, p414.
- [14] G. Rong, Proceedings of the 32<sup>nd</sup> International Conference on High Energy Physics, Beijing, China, 16-22 Aug. 2004, p1200; M. Ablikim *et al.* (BES Collaboration), Contribution paper to Lepton Photon 2005 (LP05-452).